Available online at www.sciencedirect.com
SCIENCE DIRECT®
ELSEVIER
Earth and Planetary Science Letters 7012 (2004) 1–11
EPSL
www.elsevier.com/locate/epsl

Quaternary deformation, river steepening, and heavy precipitation at the front of the Higher Himalayan ranges

Kip V. Hodges *, Cameron Wobus, Katharine Ruhl, Taylor Schildgen, Kelin Whipple

Department of Earth, Atmospheric, and Planetary Sciences, Massachusetts Institute of Technology, Cambridge, MA 02139, USA

Received 11 September 2003; received in revised form 5 January 2004; accepted 21 January 2004

Abstract

New geologic mapping in the Marsyandi Valley of central Nepal reveals the existence of tectonically significant Quaternary thrust faults at the topographic front of the Higher Himalaya. The zone of recent faulting is coincident with an abrupt change in the gradient of the Marsyandi River and its tributaries, which is thought to mark the transition from a region of rapid uplift in the Higher Himalayan ranges to a region of slower uplift to the south. Uplift of the Higher Himalaya during the Quaternary is not entirely due to passive uplift over a deeply buried ramp in the Himalayan sole thrust, as is commonly believed, but partially reflects active thrusting at the topographic front. The zone of active thrusting is also coincident with a zone of intense monsoon precipitation, suggesting a positive feedback relationship between focused erosion and deformation at the front of the Higher Himalayan ranges.

Keywords: continental tectonics; geomorphology; precipitation; erosion; Himalaya

1. Introduction

Defining the southern margin of the Tibetan Plateau, the Higher Himalayan ranges include Earth's highest mountains and deepest gorges. Their rugged topography contrasts markedly with that of the Lower Himalayan ranges farther south, which display only moderate relief and have maximum elevations of generally less than 3000 m. This distinction implies that the Higher Himalaya are being uplifted relative to the Lower Himalaya. While geodetic studies have confirmed this [1–3], the way in which differential movement between the two physiographic provinces relates to deformational structures is not well understood. The most prevalent model [3–5] holds that Holocene uplift of the Higher Himalaya is passive and related to episodes of seismic slip and interseismic strain accumulation on a deep-seated ramp in the Himalayan sole thrust (HST; Fig. 1a). In this model, no active, surface breaking thrusts occur north of the trace of the Main Frontal thrust (MFT). An alternative interpretation [6] is that the Lower Himalaya/Higher Himalaya

* Corresponding author. Tel.: +01-617-253-2927.
E-mail address: kvhodges@mit.edu (K.V. Hodges).

0012-821X/04/$ – see front matter © 2004 Published by Elsevier B.V.
doi:10.1016/S0012-821X(04)00063-9

transition – hereafter referred to as 'Physiographic Transition 2' (PT_2) for consistency with earlier work [7] – is marked by active, surface-breaking faults that root directly into the HST and accommodate differential uplift in an active way (Fig. 1b). In most sectors of the central Himalayan orogen, these hypotheses are impossible to test using geologic observations because PT_2 is covered by dense, subtropical jungle and rock exposures are limited. However, the recent construction of a road along the Marsyandi River, in the Annapurna region of central Nepal, provides unprecedented roadcut exposures across PT_2 as well as new access routes to previously unstudied riverside outcrops. Here we describe the results of detailed structural mapping along this transect (Fig. 2), which provides direct evidence for Quaternary surface-breaking deformation at PT_2.

2. Tectonic stratigraphy

Bedrock near PT_2 in the Marsyandi drainage can be separated into three units. The northernmost and structurally highest unit (the Bahundada Gneiss) includes pelitic gneisses and granites, the latter indicative of ~22–23 Ma melting during metamorphism [8,9]. It is underlain by a package of mixed rock types, the Siurun Complex. The predominate rock type in this unit is a pelitic schist, but other lithologies include granitic orthogneisses, marbles, and quartzites. The lowermost package (the Kuncha Schist) is made up almost exclusively of pelitic schists and phyllites similar in composition to the schists of the Siurun Complex.

Integrated petrologic and Th/Pb geochronologic studies by Catlos and co-workers in the

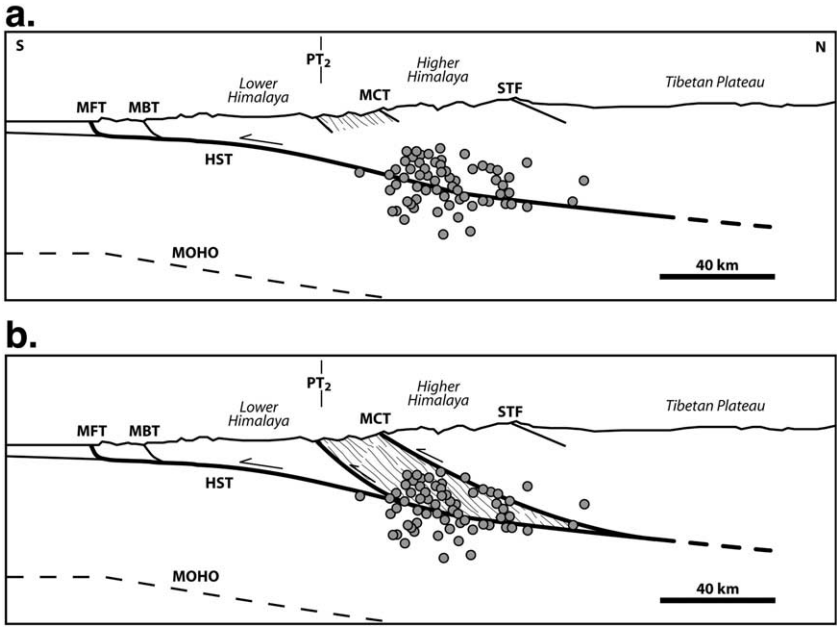

Fig. 1. Models for Holocene uplift of the Higher Himalaya and the spatial distribution of thrust activity. Crustal structure after [5,7], with earthquake hypocenters (gray circles) from [39]. Major fault systems: Himalayan Sole thrust (HST), Main Frontal thrust (MFT), Main Boundary thrust (MBT), Main Central thrust (MCT), and South Tibetan fault (STF). Patterned zone bound to the north by the MCT represents the Lesser Himalayan duplex. (a) 'Passive' model [4,5] in which uplift of the Higher Himalaya is related entirely to movement of hanging wall rocks over a ramp in the HST beneath the Lesser Himalayan–Higher Himalayan transition (PT_2). The active fault system is shown in bold. During interseismic intervals, when the HST is locked, uplift is thought to be related to strain accumulation over the ramp [3]. (b) Alternative 'active' model [6] in which uplift is related to faults that ramp to the surface near PT_2. Active faults (bold) include reactivated segments of the MCT system and both new and reactivated structures of the Lesser Himalayan duplex. Both models may be correct at different times during the Quaternary period.

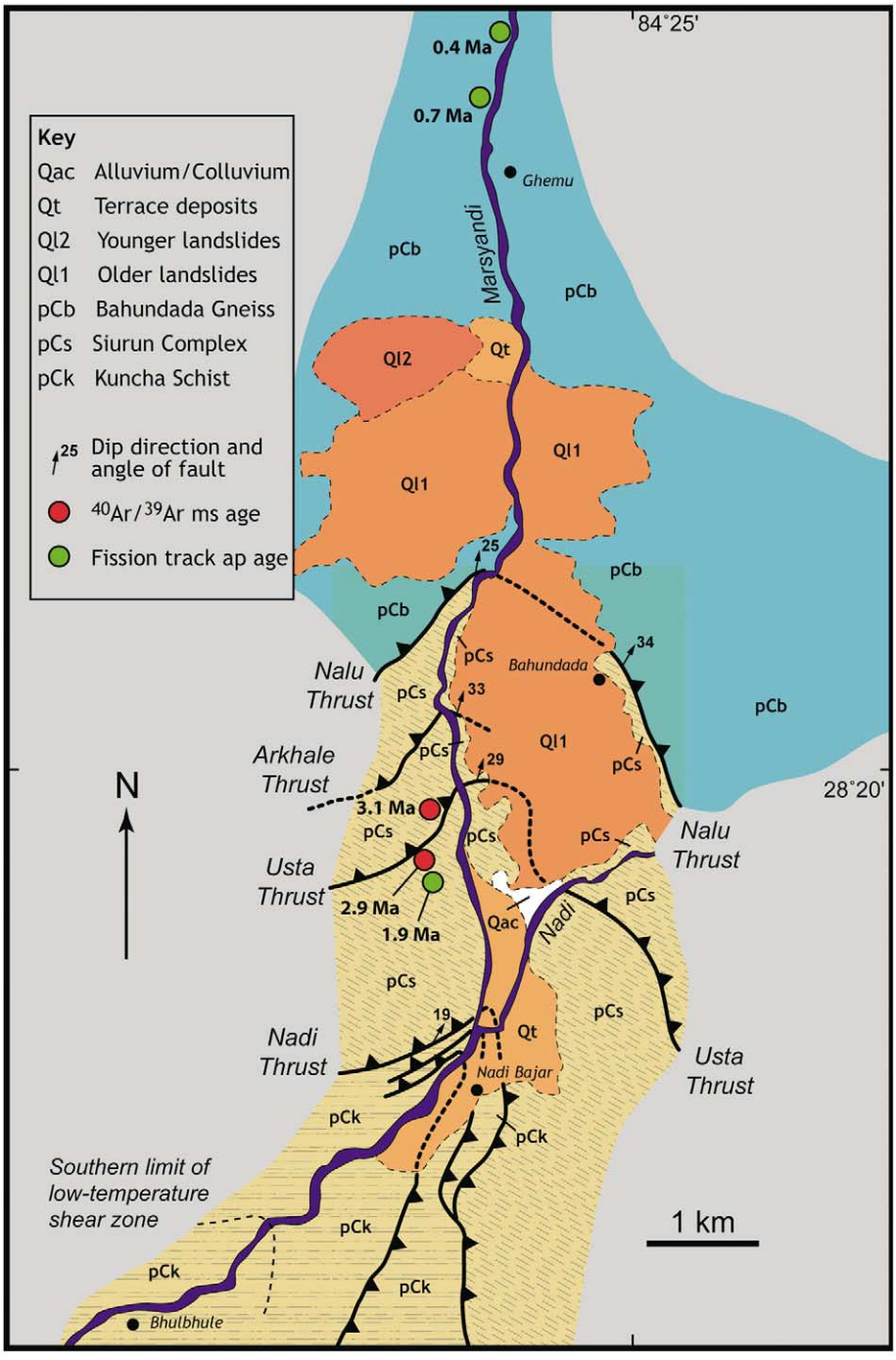

Fig. 2. Simplified geologic map of the Marsyandi River valley near PT_2. The northern boundary of the zone of intense post-Miocene deformation lies just north of the area shown in the figure. Fission-track apatite (ap) and $^{40}Ar/^{39}Ar$ muscovite (ms) cooling ages are from [15] and [13]; both references include additional data for samples collected north and south of the study area.

Marsyandi Valley [9] show that these three rock packages experienced different metamorphic histories. Both the Bahundada and Siurun units were metamorphosed to amphibolite facies, but peak pressures and temperatures were achieved at significantly different times in the two rock packages: ~750°C, 1200 MPa in the Bahundada Gneiss at ~22–23 Ma, and 600–650°C, 950–1100 MPa in the Siurun Complex at ~18 Ma. Catlos and co-workers [9] obtained no thermobarometric data for the Kuncha Schist in the area of Fig. 2, but samples collected at a somewhat deeper structural level record conditions of 550°C, 650 MPa. Significantly, 8.1–3.3 Ma Th/Pb monazite dates for the Kuncha Schist showed that metamorphism in this unit is much younger than that in the overlying Bahundada and Siurun units.

The three bedrock units are overlain by Quaternary sedimentary deposits. Although a more systematic investigation is warranted, we tentatively identify at least four separate kinds of Quaternary strata. Older and younger generations of locally derived bedrock landslide deposits (Ql1 and Ql2, respectively) have been identified based on overlap relationships. They have total volumes of up to several cubic kilometers; only the largest are shown on Fig. 2. Ql1 landslides appear stabilized by new-growth vegetation, whereas Ql2 landslides do not. In many cases, extremely steep cliffs are formed in the Ql2 landslides and they are almost certainly recent. A maximum age for the Ql2 landslide shown on Fig. 2 is suggested by the observation that it has overridden an alluvial terrace that is thought to be correlated with ~4 ka terraces further downstream [10,11]. This terrace and others in the map area consist of poorly sorted conglomerates and intercalated sandstones labeled Qt in Fig. 2. The youngest Quaternary deposits are unconsolidated sediments of alluvial and colluvial origin (Qac).

3. Deformational features

At the regional scale, the Kuncha and Siurun units correlate with what is traditionally referred to as the Lesser Himalayan sequence, while the Bahundada Gneiss correlates with the Greater Himalayan sequence [12]. The Siurun–Bahundada contact thus corresponds to the principal fault of the Main Central thrust (MCT) system, a major deformational feature that has been traced along much of the length of the Himalayan chain. Here, as is the case elsewhere in the orogen, initial MCT displacement took place in Early Miocene time [8]. However, the principal MCT fault in the Marsyandi Valley (the Nalu thrust in Fig. 2) clearly shows evidence of post-Early Miocene slip because it separates units with different metamorphic histories [9].

New exposures in the valley display two generations of fault-related fabrics that postdate Early Miocene amphibolite facies metamorphism in the Bahundada and Siurun units. The earliest includes low-temperature (greenschist facies) fabrics that persist for ~7 km upstream and downstream from the Nalu thrust in the form of numerous discrete, 1–5-m-wide shear zones that dip 30–50°N. Fabric asymmetries indicate SSW-directed, thrust-sense motion on these features. Samples of synkinematic muscovite collected from two small shear zones of this generation (Fig. 2) yielded 2.9 ± 0.1 and 3.1 ± 0.1 Ma (2σ) $^{40}Ar/^{39}Ar$ dates [13]. Since the temperature of muscovite growth during retrogression most likely was not much greater than the closure temperature for ^{40}Ar diffusion in muscovite [14], we interpret the age of the shear fabrics as ~3–4 Ma. These ductile fabrics are overprinted by brittle fabrics (breccia zones and cataclastic shear bands) along some of the largest shear zones and the Nalu thrust. Because the temperatures at which these brittle fabrics formed must have been substantially lower than the temperatures at which the ductile shear zones formed, the younger fabrics are likely to be of Pleistocene age. Direct evidence for substantial Pleistocene slip on the Nalu thrust is provided by thermochronologic data for rocks on either side of the fault in the Marsyandi Valley: apatite fission-track cooling dates from the hanging wall to the north are ≤ 0.9 Ma, whereas those from the footwall to the south are ≥ 1.9 Ma [15].

Several large, previously unidentified, moderately north-dipping thrust faults were mapped in addition to the Nalu thrust (Fig. 2). Each of these structures is marked by hydrothermal travertine

deposits, and some are conduits for active hot springs. The most significant of the newly identified faults appears to be the Nadi thrust, which juxtaposes the Siurun and Kuncha units and marks a discontinuity between rocks that experienced prograde metamorphism at different times and conditions. Major slip on the Nadi thrust postdated Late Miocene–Late Pliocene metamorphism of the Kuncha Schist and must be younger than 3.3 Ma. A minimum age is provided by the observation that the thrust does not deform ~4 ka alluvial terrace deposits.

Although the juxtaposition of rock packages with different post-Late Miocene thermal histories requires significant amounts of slip on the Quaternary faults mapped in the Marsyandi Valley, there is no way to quantify these amounts. The rocks on either side of the Nadi and Nalu thrusts belong to different tectonostratigraphic units and we have no idea what their relative lateral positions were prior to Quaternary deformation. The other major structures occur within the Siurun Complex or the Kuncha Schist, and we do not know the internal stratigraphy of either well enough to permit reconstruction of the pre-deformational state.

4. Geomorphologic evidence for differential uplift across PT_2

The zone of thrust faults shown in Fig. 2 corresponds to PT_2 as broadly defined by topographic profiles drawn through the Annapurna region, but an important question remains: do they accommodate modern differential uplift across the transition? To address this question, we examined longitudinal profiles of the Marsyandi and its tributaries in the vicinity of PT_2. Empirical studies [16–18] have shown that the local channel slope (S) of a stream is generally a power law function of the stream drainage area (A): $S = k_s A^{-\theta}$, where k_s is the steepness index, and θ is the concavity index. (Note that θ is dimensionless and k_s has units of $m^{2\theta}$.) Regression analysis of logS vs. logA for natural streams offers a straightforward way to explore the possibility of along-stream changes in bedrock uplift rates because, in theory, the two derived indices vary in a predictable way with changing rates and patterns of uplift [19–22]. For example, while along-stream variations in channel width, erosional mechanism, and rock competency may complicate the relationship [21,23–25], it is generally the case that higher values of k_s correlate with higher surface uplift rates [20,26].

Less than 100 km east of the study area, Wobus et al. [27] analyzed the longitudinal profiles of rivers crossing PT_2 where it lies 20–30 km south of the trace of the principal fault of the MCT system. They found an abrupt decrease in k_s downstream of PT_2 that was interpreted as resulting from much higher uplift rates in the Higher Himalaya than in the Lower Himalaya. A discontinuity in the pattern of $^{40}Ar/^{39}Ar$ muscovite cooling dates at PT_2 (much younger dates to the north than to the south) reinforced this interpretation. Here we employ a similar geomorphologic approach to evaluate whether or not river profiles change substantially across the zone of Quaternary thrusting in Fig. 2.

Our analysis is based on data extracted from a 90-m digital elevation model. Because empirical studies and theory suggest that the concavity index typically varies within a relatively restricted range in active orogens (~0.3–0.6; [20,26,28]), we elected to assume a value of 0.45 for θ (for consistency with the earlier work of Wobus et al. [27]) and explore downstream variations in k_s through least-squares regression of logS as a linear function of logA. Steepness indices were calculated along the length of the channel based on the regression of data within a window including logS and logA values roughly 5 km upstream and 5 km downstream of each point; in every case, the slope of the regression line was fixed by the assumption of $\theta = 0.45$.

In theory, steady-state river concavity should change if precipitation varies markedly along the stream course as a consequence of orographic effects [28]. By assuming no change in θ, we force any effects of variable precipitation to be manifested as variations in k_s. As we discuss in more detail later in this paper, strong, orographically controlled variations in precipitation do occur across the study area [29], but these variations

do not correlate in any apparent way with calculated variations in k_s. Regardless, different approaches to the regression analysis of logS and logA would not change the basic conclusion of our analysis: there is a sharp transition in channel steepness across the zone of post-Miocene deformation defined by geologic mapping (Figs. 3 and 4a).

Upstream of its confluence with the Nadi Khola, the Marsyandi is characterized by very high k_s (>450 m$^{0.9}$). Downstream of the confluence, steepness values drop off rapidly to moderate levels (<250 m$^{0.9}$). The Nadi Khola profile is steep along its entire length, suggesting that this tributary drainage lies exclusively in a zone of high uplift rate. In contrast, the Kisanti Khola has moderate k_s along its entire length, suggesting that its drainage basin is south of the region of rapid uplift. All other streams in Fig. 3, like the Marsyandi, have upper reaches that are characterized by high k_s and lower reaches with k_s values that are typically lower by a factor of two. The downstream limit of very high k_s can be defined to within ~1–2 km in each of these drainages

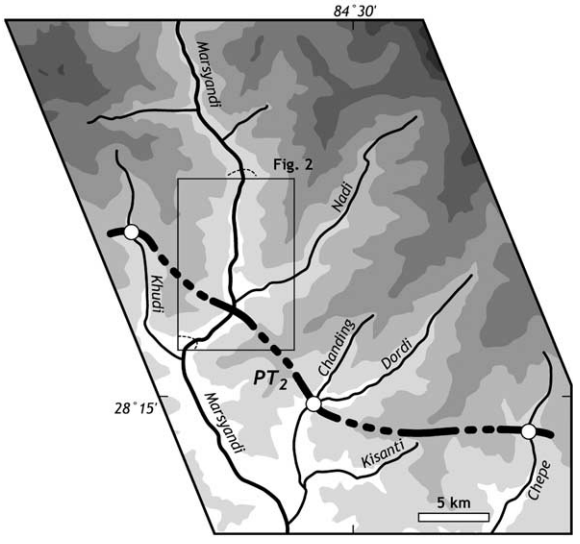

Fig. 3. PT_2 as defined by stream profiles for the Marsyandi River and major tributaries. Shading indicates topography in 1000-m intervals (unpatterned areas below 1000-m elevations, darkest patterned areas above 7000 m). Thick line (dashed where approximately located) marks the southern boundary of the region where drainages typically have very high k_s (>450 m$^{0.9}$ for $\theta = 0.45$). Open circles mark distinct knickpoints at this boundary. The area of Fig. 2 is indicated by a box. Thin dashed lines north of and within the box mark the northern and southern boundaries of the zone of intense post-Miocene deformation.

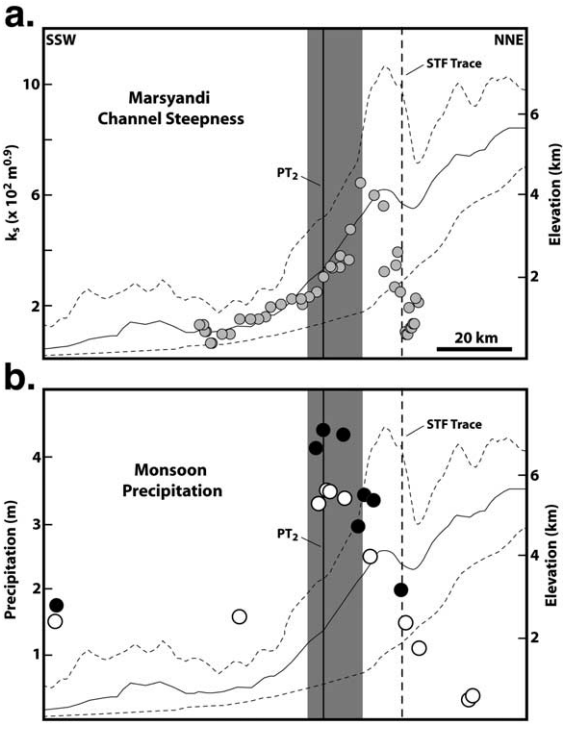

Fig. 4. (a) Spatial relationships among topography, river steepness, and deformational features in the Annapurna Range. Thin solid line indicates mean elevations along a ~50-km-wide, SSW–NNE transect orthogonal to the range front, with dashed lines indicating the minimum–maximum envelope [15]; scale shown on right. Shaded circles indicate values of k_s (scale shown on left) based on slope–drainage area data for the Marsyandi trunk stream at 5-km intervals along its course; each circle is the result of log–log regressions of data over a 10-km window, with an assumed concavity (θ) of 0.45. Because the river does not run SSW–NNE along its entire course, each point has been projected to the line of section. Shaded region indicates the boundaries of the Quaternary deformation zone described in the text. Thick vertical line indicates the position of PT_2 as defined by stream profile analysis. Dashed line marks the approximate trace of the basal detachment of the South Tibetan fault system in the area [51,52]. (b) Monsoon rainfall distribution across the Annapurna Range [15,29], projected to the same line of section shown in frame (a). Circles indicate average annual monsoon precipitation, as measured at meteorological stations on ridges (filled) and in valleys (open), projected onto the line of section; scale shown on left.

and, in some cases, it corresponds to a distinct knickpoint in the stream gradient. It is highly unlikely that this boundary marks a change in the erosional resistance of the bedrock because the predominant lithologies on both sides are pelitic schist and phyllite with comparable strength. Instead, we interpret the boundary as the southern limit of the rapidly uplifting Higher Himalaya. Given the capacity of river channel geometry to respond quickly to changes in bedrock uplift rate [30,31], the uplift discontinuity in the Marsyandi area almost certainly has been active within the past 100 000 years. In the Marsyandi Valley, the discontinuity lies close to the surface trace of the Nadi thrust, suggesting that this feature may be the principal locus of Quaternary shortening in the study area.

5. Implications

In a recently published kinematic model for deformation in the central Nepalese Himalaya, Robinson and co-workers [32] invoked the development of a thrust duplex within the Lesser Himalayan sequence to explain the Late Miocene–Pliocene metamorphism documented by Catlos and co-workers [9] in the Annapurna region. Although the structural configuration inferred in that model is based on field work in western Nepal, our mapping in the Marsyandi drainage confirms the existence of significant thrust faults within the Lesser Himalayan sequence in central Nepal. More importantly, our work indicates that such structures have been active in the recent geologic past.

The results reported here challenge a number of widely held beliefs regarding post-Miocene deformation in the central Himalaya. The traditional view of the structural development of the Himalaya is that active faulting propagated from north to south with time: the MCT system, active in early Miocene time, was succeeded by the Pliocene Main Boundary thrust (MBT) system, which was succeeded in turn by the active Main Frontal thrust (MFT) system [12,33,34]. Even recent models that recognize the significance of faulting within the Lower Himalaya between the MCT and MBT emphasize the N-to-S progression of faulting [32]. While the evidence for a N-to-S trend in the age of fault initiation is compelling, our work and other recent studies [7,9,27,35] suggest that the pattern of active faulting on these structures has been much more complicated over the past 4 Ma. For example, brittle and low-temperature thrust structures in Fig. 2 were active subsequent to development of the MBT and MFT systems in this part of the orogen [7].

The total percentage of Pliocene–Recent convergence between India and Eurasia accommodated by such out-of-sequence structures remains unclear, however. Lavé and Avouac [36] presented persuasive geomorphologic evidence that the MFT in central Nepal experienced $\sim$2 cm/yr shortening averaged over the past 10 000 years. Since this rate is comparable to the modern rate of convergence across this sector of the Himalaya [3,37,38], one reasonable interpretation (Fig. 1a) is that virtually all of the Holocene shortening across the central part of the orogen has been accommodated by slip on the HST with none of it being partitioned to thrusts farther north [31]. Given the direct evidence for substantial Quaternary slip at PT_2 presented in this paper, this interpretation can be correct only if most of the deformation on structures such as those shown in Fig. 2 is older than $\sim$10 000 years. While this would be consistent with the available age constraints for Quaternary deformational structures in the Marsyandi drainage, several lines of evidence suggest that these structures may still be active. For example, large Holocene landslides are localized near PT_2 in the Annapurna Range, as evidenced by units Ql1 and Ql2 in Fig. 2. These features are likely to have been caused by local seismic activity. The epicenters of most earthquakes in the Himalayan realm lie at or north of PT_2 [4,39]; their positions and seismic character are equally consistent with the traditional view [40] that they are related to slip on the down-dip projection of the MFT (Fig. 1a), or with the alternative view that they are related to slip on out-of-sequence faults that project to the surface near PT_2 (Fig. 1b). Two recent, large earthquakes on the HST – the 1991 Uttarkashi (m_b 6.6) and 1999 Chamoli (m_b 6.3) events in the northwestern In-

dian Himalaya – were accompanied by large aftershocks indicative of slip on relatively steep, north-dipping thrust faults in the Lower Himalaya [41,42], structures that are in a structural position analogous to the Quaternary faults mapped in the Marsyandi Valley.

If substantial slip has occurred on out-of-sequence thrust faults in the Himalaya over the past 10 000 years, why do the observations of Lavé and Avouac [36] suggest that shortening across the MFT is alone sufficient to account for all of the convergence across the Himalaya at this longitude? In asking such a question, it is important to recognize that the relative contributions of out-of-sequence deformation and deformation at the Himalayan front are likely to have varied in space and time over the Pliocene–Recent interval, as noted by Lavé and Avouac [31]. For example, while the work of Lavé and Avouac [36] implies active shortening across the MFT in central Nepal at a rate of ~21 mm/a, similar work by Wesnousky et al. [43] in northwest India yielded an estimate of ~14 mm/a. Moreover, these geomorphologic estimates of shortening across the MFT have unavoidable uncertainties of 20–40%, and geodetic estimates of convergence across the Himalaya have significant uncertainties as well. As a consequence, the estimates of MFT shortening and cross-Himalayan convergence easily could differ by several millimeters per year. If out-of-sequence thrusts have dips such as those shown in Fig. 2, they could accommodate significant slip that might simply be lost in the uncertainty.

Some amount of N–S shortening on out-of-sequence structures may be balanced by an equivalent amount of N–S extension on orogen-parallel normal faults north of the zone of out-of-sequence thrusting and south of the Tibetan Plateau. Several Quaternary normal faults with appropriate orientations have been identified between PT_2 and the Himalayan crest in central Nepal and the northwest Indian Himalaya [35,44], but the largest concentration of candidate structures occurs near the range crest as part of the South Tibetan fault (STF) system [45]. This fault system, which helps define the upper boundary of the Greater Himalayan sequence (Fig. 1), developed in Miocene time, but various lines of evidence suggest that some faults of the STF have been active in the Quaternary Period over broad regions of the Himalaya [7]. For example, some of the most compelling evidence for Quaternary activity on the STF system comes from the western Annapurna Range, only about 75 km northwest the area shown in Fig. 2 [46].

In our view, the evidence presented here and elsewhere [27,35] for out-of-sequence Quaternary faulting does not preclude the possibility that seismic slip and interseismic strain accumulation on a deep-seated ramp in the Himalayan sole thrust played an important role in Holocene uplift of the Higher Himalaya [3–5]. However, current 'passive' models for Higher Himalayan uplift (e.g. [3–5]) should be modified to account for the additional effects of out-of-sequence thrusting. One reason why out-of-sequence thrusts may develop in the vicinity of PT_2 was suggested by Hodges et al. [7]. Compared to its surroundings, the Tibetan Plateau is characterized by excess gravitational potential energy that can be dissipated effectively through the removal of mass from the Himalayan ranges through erosion. The efficiency of this dissipative process depends on the rate at which material is transported to the Himalaya through tectonic processes and the rate at which erosional processes can remove material. If erosion rates increase with increasing relief, as is commonly believed, the efficiency of excess gravitational potential energy dissipation in the Himalaya is optimized when the efficiency of differential uplift between the Higher and Lower Himalaya is greatest. As a consequence, the trend toward higher dissipative efficiency would favor out-of-sequence thrusting near PT_2, which provides a more efficient mechanism for differential uplift between the Higher and Lower Himalaya than does the passive translation of the Greater Himalayan and Lesser Himalayan sequences over a deep-seated ramp. Such logic leads to the prediction that orogenic systems with strong orographic forcing of precipitation should display out-of-sequence thrusts in regions of concentrated erosion, a notion that is strongly supported by geodynamic modeling studies of the Himalaya [47].

In this regard, we note a remarkable spatial relationship among the patterns of young deformation, river channel morphology, and precipitation in the Annapurna region. When projected on a section orthogonal to the trend of the Annapurna Range (Fig. 4a), k_s values for the Marsyandi channel are anomalously high in a zone bounded to the north by the trace of the South Tibetan fault (STF) system and to the south by PT_2. In light of previously published evidence for Quaternary activity on the STF system in the Annapurna Range and the geologic mapping presented here, we interpret this pattern as evidence that the zone between the STF trace and PT_2 has experienced more rapid uplift than the regions to the north or south as a consequence of simultaneous slip on Quaternary thrust and normal faults. Moreover, the zone of accelerated uplift appears to correspond to a zone of anomalously high rainfall during the summer monsoon over the past few years (Fig. 4b [15,29]). The highest precipitation, nearly twice that which falls to the north or south of the band, is centered on the position of PT_2 as shown in Fig. 3. This observation supports models of Himalayan tectonics that relate the southward extrusion of Tibetan middle–lower crust to focused erosion at the front of the Higher Himalayan ranges [7,27,47–49]. A striking spatial correlation of heavy rainfall and active deformation suggests that precipitation patterns may strongly influence active faulting patterns in this region, and that these patterns, in turn, may largely dictate the geomorphology of its river systems.

As noted by Molnar [50], the relative impact of climatic and tectonic processes on erosion in active orogens remains controversial. Based on differences between the patterns of monsoon precipitation and young fission-track apatite cooling dates in the Marsyandi drainage, Burbank and co-workers [15] argued that monsoon precipitation and erosion are decoupled, and they concluded that large-scale deformation, rather than precipitation, dictates the pattern of erosion. However, we have discovered a correlation between Quaternary deformation patterns and precipitation patterns in the same study area; if deformation and precipitation are coupled, and if Burbank and co-workers are correct that tectonics and erosion are coupled, then it seems inescapable that, at some level, precipitation and erosion are coupled as well. It may be difficult to evaluate the exact nature and degree of such coupling through local field studies such as ours or that of Burbank et al. [15] because the length scales over which the different processes operate may be substantially different from one another. In our opinion, the popular debate about whether tectonics or climate 'controls' erosion in active orogens is less important than finding the answer to a more fundamental question: why do orogenic systems 'self-organize' such that all three processes – deformation, precipitation, and erosion – appear to be coordinated?

We agree with Molnar's assertion [50] that a better theoretical framework is necessary before we can really understand how climate, erosion, and tectonics relate to one another, but the development of more comprehensive databases is just as important if we are to test the viability of new theories that might arise. Regionally extensive data pertinent to long- and short-term erosion rates are unavailable for most active orogens. While observing platforms in space provide images of on-going atmospheric processes with unprecedented scope, the meteorological data are generally of too low a resolution to match the scale of existing datasets for erosional processes. We have been fortunate in the Marsyandi drainage to have precipitation data over the appropriate length scale to address some of critical questions about climate, tectonics, and erosion, but even there we cannot be sure that we are comparing processes in an appropriate way. For example, the deformational structures and river channels described in this report were produced over tens of thousands of years, but the precipitation data shown in Fig. 4a represent only a 4-yr record. Might the apparent correlation between deformation and heavy precipitation fall apart if we were comparing the two processes over the same time scale? In order to answer this question, it is imperative to develop and maintain long-term environmental monitoring networks in a variety of settings. The challenge before us is to integrate both well-grounded theory and more comprehensive datasets to determine whether apparent rela-

tionships among processes like deformation, precipitation, and erosion are mere coincidence, or are instead telling us something fundamental about how orogenic systems evolve.

Acknowledgements

This research was funded by a NSF grant to K.V.H. as part of the Continental Dynamics project (Geomorphic–Geodynamic Coupling at the Orogen Scale). We thank Ana Barros, Ann Blythe, Doug Burbank, Beth Pratt-Sitaula, and Jaakko Putkonen for sharing their data and thoughts on the geology and climate of the central Himalaya, and Chris Beaumont, Don Fisher, and Gerard Roe for reviewing an earlier version of the manuscript. Tank Prasad Ojha and the crew of Himalayan Experience provided invaluable logistical assistance.*[BOYLE]*

References

[1] M.E. Jackson, R. Bilham, 1991–1992 GPS measurements across the Nepal Himalaya, Geophys. Res. Lett. 21 (1994) 1169–1172.
[2] M. Jackson, R. Bilham, Constraints on Himalayan deformation inferred from vertical velocity fields in Nepal and Tibet, J. Geophys. Res. 99 (1994) 13897–13912.
[3] R. Bilham, K. Larson, J. Freymuller, P.I. Members, GPS measurements of present-day convergence across the Nepal Himalaya, Nature 386 (1997) 61–64.
[4] M.R. Pandey, R.P. Tandukar, J.P. Avouac, J. Lavé, J.P. Massot, Interseismic strain accumulation on the Himalayan crustal ramp (Nepal), Geophys. Res. Lett. 22 (1995) 751–754.
[5] R. Cattin, J.P. Avouac, Modeling mountain building and the seismic cycle in the Himalaya of Nepal, J. Geophys. Res. 105 (2000) 13389–13407.
[6] L. Seeber, V. Gornitz, River profiles along the Himalayan arc as indicators of active tectonics, Tectonophysics 92 (1983) 335–367.
[7] K.V. Hodges, J.M. Hurtado, K.X. Whipple, Southward extrusion of Tibetan crust and its effect on Himalayan tectonics, Tectonics 20 (2001) 799–809.
[8] M.E. Coleman, U–Pb constraints on Oligocene–Miocene deformation and anatexis within the central Himalaya, Marsyandi valley, Nepal, Am. J. Sci. 298 (1998) 553–571.
[9] E.J. Catlos, T.M. Harrison, M.J. Kohn, M. Grove, F.J. Ryerson, C.E. Manning, B.N. Upreti, Geochronologic and thermobarometric constraints on the evolution of the Main Central Thrust, central Nepalese Himalaya, J. Geophys. Res. 106 (2001) 16177–16204.
[10] H. Yamanaka, Radiocarbon ages of upper Quaternary deposit in central Nepal and their geomorphological significance, Sci. Rep. Tohoku Univ. Ser. 7 (1982) 46–60.
[11] B. Pratt-Sitaula, D.W. Burbank, A. Heimsath, T. Ojha, Landscape disequilibrium on 1,000 to 10,000 year scales, Marsiyandi River, Nepal, Geomorphology (in press).
[12] K.V. Hodges, Tectonics of the Himalaya and southern Tibet from two perspectives, Geol. Soc. Am. Bull. 112 (2000) 324–350.
[13] R.M. Edwards, $^{40}Ar/^{39}Ar$ geochronology of the Main Central thrust (MCT) region: Evidence for Late Miocene to Pliocene disturbances along the MCT, Marsyangdi River valley, west-central Nepal Himalaya, J. Nepal Geol. Soc. 10 (1995) 41–46.
[14] K.V. Hodges, Geochronology and thermochronology in orogenic systems, in: R.L. Rudnick (Ed.), The Crust, Treatise on Geochemistry 3, Elsevier Science, Amsterdam, 2003, pp. 263–292.
[15] D.W. Burbank, A.E. Blythe, J.K. Putkonen, B.A. Pratt-Sitaula, E.J. Gabet, M.E. Oskin, A.P. Barros, T.P. Ojha, Decoupling of erosion and precipitation in the Himalaya, Nature 426 (2003) 652–655.
[16] J.T. Hack, Stream profile analysis and stream-gradient index, J. Res. US. Geol. Surv. 1 (1973) 421–429.
[17] J.J. Flint, Stream gradient as a function of order, magnitude, and discharge, Water Resourc. Res. 10 (1974) 969–973.
[18] A.D. Howard, G. Kerby, Channel changes in badlands, Geol. Soc. Am. Bull. 94 (1983) 739–752.
[19] K.X. Whipple, G.E. Tucker, Dynamics of the stream-power river incision model: Implications for height limits of mountain ranges, landscape response timescales, and research needs, J. Geophys. Res. 104 (1999) 17661–17674.
[20] N. Snyder, K. Whipple, G. Tucker, D. Merritts, Landscape response to tectonic forcing: Digital elevation model analysis of stream profiles in the Mendocino triple junction region, northern California, Geol. Soc. Am. Bull. 112 (2000) 1250–1263.
[21] K.X. Whipple, G.E. Tucker, Implications of sediment-flux-dependent incision models for landscape evolution. J. Geophys. Res. 107 (2002) doi: 1029/2000JB000044.
[22] K.X. Whipple, Bedrock rivers and the geomorphology of active orogens, Annu. Rev. Earth Planet. Sci. 32 (2004) 151–185.
[23] L. Sklar, W.E. Dietrich, River longitudinal profiles and bedrock incision models: Stream power and the influence of sediment supply, in: K.J. Tinkler, E.E. Wohl (Eds.), Rivers over Rock: Fluvial Processes in Bedrock Channels, Geophys. Monogr. Ser. 107, AGU, Washington, DC, 1998, pp. 237–260.
[24] K.X. Whipple, R.S. Anderson, G.S. Dick, River incision into bedrock: Mechanics and relative efficacy of plucking, abrasion, and cavitation, Geol. Soc. Am. Bull. 112 (2000) 490–503.
[25] D.R. Montgomery, N. Finnegan, A. Anders, B. Hallet,

Downstream adjustment of channel width to spatial gradients in rates of rock uplift at Namche Barwa. Geol. Soc. Am. Abstr. Progr., 2002.
[26] E. Kirby, K. Whipple, Quantifying differential rock-uplift rates via stream profile analysis, Geology 29 (2001) 415–418.
[27] C.W. Wobus, K.V. Hodges, K.X. Whipple, Has focused denudation sustained active thrusting at the Himalayan topographic front?, Geology 31 (2003) 861–864.
[28] G.H. Roe, D.R. Montgomery, B. Hallet, Effects of orographic precipitation variations on the concavity of steady-state river profiles, Geology 30 (2002) 143–146.
[29] A.P. Barros, M. Joshi, J. Putkonen, D.W. Burbank, A study of the 1999 monsoon rainfall in a mountainous region in Central Nepal using TRMM products and rain-gauge observations, Geophys. Res. Lett. 27 (2000) 3683–3686.
[30] K.X. Whipple, Fluvial landscape response time: How plausible is steady-state denudation?, Am. J. Sci. 301 (2001) 313–325.
[31] J. Lavé, J.P. Avouac, Fluvial incision and tectonic uplift across the Himalayas of central Nepal, J. Geophys. Res. 106 (2001) 26561–26591.
[32] D.M. Robinson, P.G. DeCelles, C.N. Garzione, O.N. Pearson, T.M. Harrison, E.J. Catlos, Kinematic model for the Main Central Thrust in Nepal, Geology 31 (2003) 359–362.
[33] A. Gansser, Geology of the Himalayas, Wiley Interscience, London, 1964, 289 pp.
[34] P. LeFort, Himalayas: The collided range. Present knowledge of the continental arc, Am. J. Sci. 275-A (1975) 1–44.
[35] B. Grasemann, E. Draganits, C. Janda, C. Hager, J.-C. Vannay, Active exhumation of a high-grade asymmetric dome in the Sutlej valley (NW-Himalayas, India). Geol. Soc. Am. Abstr. Progr. 34(6), 2002.
[36] J. Lavé, J.P. Avouac, Active folding of fluvial terraces across the Siwalik Hills, Himalayas of central Nepal, J. Geophys. Res. 105 (2000) 5735–5770.
[37] F. Jouanne, J.L. Mugnier, M.R. Pandey, J.F. Gamond, P. LeFort, L. Serrurier, C. Vigny, J.P. Avouac, Oblique convergence in the Himalayas of western Nepal deduced from preliminary results of GPS measurements, Geophys. Res. Lett. 26 (1999) 1933–1936.
[38] K. Larson, R. Bürgmann, R. Bilham, J. Freymueller, Kinematics of the India–Eurasia collision zone from GPS measurements, J. Geophys. Res. 104 (1999) 1077–1093.
[39] M.R. Pandey, R.P. Tandukar, J.P. Avouac, J. Vergne, T. Héritier, Seismotectonics of the Nepal Himalaya from a local seismic network, J. Asian Earth Sci. 17 (1999) 703–712.
[40] L. Seeber, J.G. Armbruster, Great detachment earthquakes along the Himalayan arc and long-term forecasting, in: D.W. Simpson, P.G. Richards (Eds.), Earthquake Prediction: An International Review, Maurice Ewing Series 4, Am. Geophys. Union, Washington, DC, 1981, pp. 259–277.
[41] F. Cotton, M. Campillo, A. Deschamps, B.K. Rastogi, Rupture history and seismotectonics of the 1991 Uttarkashi, Himalaya earthquake, Tectonophysics 258 (1996) 35–51.
[42] S.K. Nath, P. Sengupta, J.R. Kayal, Determination of S-wave site response in the Garhwal Himalaya from the aftershock sequence of the 1999 Chamoli earthquake, Bull. Seismol. Soc. Am. 92 (2002) 1072–1081.
[43] S.G. Wesnousky, S. Kumar, R. Mohindra, V.C. Thakur, Uplift and convergence along the Himalayan frontal thrust of India, Tectonics 18 (1999) 967–976.
[44] T. Nakata, Active faults of the Himalaya of India and Nepal, in: L.L. Malinconico, R.J. Lillie (Eds.), Tectonics of the Western Himalayas, Geol. Soc. Am. Spec. Pap. 232, Boulder, CO, 1989, pp. 243–264.
[45] B.C. Burchfiel, Z. Chen, K.V. Hodges, Y. Liu, L.H. Royden, C. Deng, J. Xu, The South Tibetan detachment system, Himalayan Orogen: Extension contemporaneous with and parallel to shortening in a collisional mountain belt, Geol. Soc. Am., Boulder, CO, 1992, 41 pp.
[46] J.M. Hurtado, K.V. Hodges, K.X. Whipple, Neotectonics of the Thakkhola Graben and implications for Recent activity on the South Tibetan Fault System in the central Nepalese Himalaya, Geol. Soc. Am. Bull. 113 (2001) 222–240.
[47] C. Beaumont, R.A. Jamieson, M.H. Nguyen, B. Lee, Himalayan tectonics explained by extrusion of a low-viscosity crustal channel coupled to focused surface denudation, Nature 414 (2001) 738–742.
[48] D. Grujic, L.S. Hollister, R.R. Parrish, Himalayan metamorphic sequence as an orogenic channel; insight from Bhutan, Earth Planet. Sci. Lett. 198 (2002) 177–191.
[49] R.C. Theide, B. Bookhagen, J.R. Arrowsmith, E.R. Sobel, M.R. Strecker, Climatic control on areas of rapid exhumation along the southern Himalayan front. Earth Planet. Sci. Lett. (in press).
[50] P. Molnar, Nature, nurture and landscape, Nature 426 (2003) 612–614.
[51] K.V. Hodges, R.R. Parrish, M.P. Searle, Tectonic evolution of the central Annapurna Range, Nepalese Himalayas, Tectonics 15 (1996) 1264–1291.
[52] M.E. Coleman, K.V. Hodges, Contrasting Oligocene and Miocene thermal histories from the hanging wall and footwall of the South Tibetan detachment in the central Himalaya from $^{40}Ar/^{39}Ar$ thermochronology, Marsyandi Valley, central Nepal, Tectonics 17 (1998) 726–740.